Growth of {Tb 3 }[Sc 2−x Lu x](Al 3)O 12 Single Crystals for Visible−Infrared Optical Isolators

DATASET *in* CRYSTAL GROWTH & DESIGN · AUGUST 2010

Impact Factor: 4.89 · DOI: 10.1021/cg100277w

DOI: 10.1021/cg100277w

CRYSTAL GROWTH & DESIGN Article
XXXX, Vol. XXX
000–000

Growth of $\{Tb_3\}[Sc_{2-x}Lu_x](Al_3)O_{12}$ Single Crystals for Visible-Infrared Optical Isolators

Kiyoshi Shimamura,*[,†,‡] Takayuki Kito,[†] Elias Castel,[†] Anastasiya Latynina,[†] Pablo Molina,[†] Encarnación G. Víllora,[†,‡] Prakasam Mythili,[‡] Philippe Veber,[‡] Jean-Pierre Chaminade,[‡] Akiharu Funaki,[†,∥] Tsubasa Hatanaka,[†,∥] and Kunihiro Naoe[∥]

[†]*National Institute for Materials Science, 1-1 Namiki, Tsukuba 305-0044, Ibaraki, Japan,*
[‡]*Institut de Chimie de la Matière Condensée de Bordeaux (ICMCB-CNRS), Université de Bordeaux, 87 Avenue du Docteur Albert Schweitzer, 33608 Pessac cedex, France, and*
[∥]*Fujikura Co., Ltd., 1440 Mutsuzaki, Sakura, Chiba 285-8550, Japan*

Received March 1, 2010; Revised Manuscript Received May 24, 2010

ABSTRACT: $\{Tb_3\}[Sc_{2-x}Lu_x](Al_3)O_{12}$ crystals have been grown and investigated for the first time for magneto-optical applications. $Tb_3Al_5O_{12}$ exhibits the best magneto-optical features; however, its incongruent melting nature has led to the industrial use of $Tb_3Ga_5O_{12}$. $Tb_3Sc_2Al_3O_{12}$ had been proposed as an alternative to $Tb_3Al_5O_{12}$, but unfortunately its growth also presents several drawbacks. The present investigation shows that by the isovalent substitution of Sc^{3+} by Lu^{3+} in the octahedral site of the garnet structure, it is possible to improve the growth characteristics while preserving the superior magneto-optical properties. We demonstrate that $\{Tb_3\}[Sc_{2-x}Lu_x](Al_3)O_{12}$ crystals show a higher visible transparency and a larger Faraday rotation than $Tb_3Ga_5O_{12}$ crystals. $\{Tb_3\}[Sc_{2-x}Lu_x](Al_3)O_{12}$ is therefore a very promising material in particular for new magneto-optical applications in the visible-near IR wavelength region.

Introduction

Faraday isolators (FIs) are fundamental components used in advanced optical communications, high-power laser machinery, etc. FIs prevent optical feedback, which causes parasitic oscillations in amplifier systems or frequency instabilities in laser diodes. Faraday crystals rotate 45° the polarization plane of the passing light and further 45° the reflected light, so that the latter can be eliminated with a polarizer. Yttrium–iron garnet, $Y_3Fe_5O_{12}$ (YIG), is so far the most commonly used crystal in FIs. It is characterized by a high transparency in the IR region, a large Faraday rotation angle, and a low saturation magnetization. However, YIG cannot be used at shorter wavelengths (< 1100 nm) due to its poor transparency.

New magneto-optical crystals, highly transparent in the UV-Visible-near IR region, are needed as optical isolators operating at wavelengths below 1100 nm in advanced optical data-storage systems, laser machinery, high-precision laser measurements, etc. Materials under consideration are based on rare-earth (RE) garnet single crystals. These are optically isotropic thanks to the cubic symmetry, and their Faraday rotation is essentially paramagnetic, caused by the 4f-4f5d transition of RE^{3+} ions.[1] Tb^{3+} yields to the largest Faraday rotation, so that electric dipole contribution of Tb^{3+} dominates even over that of Fe^{3+} in magnetic terbium–iron garnet.[2] The magnetic component coming from Tb^{3+} depends on the host material, which influences the lowest and first excited multiplet states of the Tb^{3+}free ion, $^7F_6$ and $^7F_5$, respectively. Complex theoretical approaches have been done through the perturbation Hamiltonian, which takes into account the spin–orbit coupling, the crystal field, and the superexchange interaction.[3]

Among the transparent paramagnetic materials, terbium–aluminum garnet, $Tb_3Al_5O_{12}$ (TAG), has been reported to show the best properties, namely, a high transparency and a high Verdet constant.[4,5] However, the incongruent melting nature of TAG has impeded so far the growth of industrially practicable crystals.[6] With the lack of TAG, FIs for high-power laser machinery are made with terbium-gallium garnet,[7] $Tb_3Ga_5O_{12}$ (TGG), which melts congruently at approximately 1825 °C. Although TGG can be synthesized by the Czochralski (Cz) technique, its growth is not exempt of difficulties. The decomposition and evaporation of gallium-sesquioxide from the melt lead to a continuous shift of (a) the melting point and (b) the composition of the crystal.[8]

An intermediate solution has been the attempted growth of TAG–TGG mixed crystals ($Tb_3Ga_{5-x}Al_xO_{12}$ with $x < 35$ at%).[9] Even with a relative small substitution of Ga by Al, Al_{Ga} presumably at the tetrahedral site, the Faraday rotation angle considerably increases, reaching values comparable to that of pure TAG. There is, however, no evidence that these kinds of mixed crystals have been further considered.

Another approach to overcome the growth difficulties encountered in this family of garnets is the substitution of the ion in the octahedral site. For example, by the incorporation of Sc^{3+} in the octahedral site in some garnets, the different polyhedral sizes could be equilibrated in order to favor the synthesis of single crystals.[10,11] Further, other studies have shown that many trivalent rare-earth (RE), in spite of their relatively large ionic radius, can occupy both dodecahedral and octahedral sites in gallium garnets.[12,13] Among the RE atoms, Lu^{3+} was even found to be able to form pure $Nd_3Lu_2Ga_3O_{12}$ compound, which was attributed to the fact that Lu^{3+} has the smallest ionic radius among RE elements.

In this investigation, we present an approach to overcome the growth difficulties of TAG substituting $[Sc_{2-x}Lu_x]$ for $[Al_2]$, thus yielding $\{Tb_3\}[Sc_{2-x}Lu_x](Al_3)O_{12}$ (TSLAG). Lu^{3+} has a larger ionic radius than Sc^{3+}, but still much smaller than Tb^{3+}, so that both are expected to enter into the octahedral site. By this it is possible to engineer the sites of the garnet

*To whom correspondence should be addressed. E-mail: SHIMAMURA.Kiyoshi@nims.go.jp, Tel: +81-29-860-4692. Fax: +81-29-851-6159.

Figure 1. Photograph of $Tb_3Sc_2Al_3O_{12}$ single crystal and the remaining melt.

structure to matching cationic sizes that will favor a congruent growth of TSLAG, while preserving the properties of TAG. In order to study these issues, several TSLAG crystals were grown by the Cz technique. The composition of the crystals was determined by chemical analysis and correlated with Rietveld refinements (RR) of the crystallographic structure. Finally, the magneto-optical properties are discussed.

Experimental Section

Nominal $\{Tb_3\}[Sc_{2-x}Lu_x](Al_3)O_{12}$ crystals with $x = 0$, 0.05, 0.1, and 0.2 were grown by the Cz technique. As starting materials, commercial oxides of Tb_4O_7, Sc_2O_3, Lu_2O_3, and Al_2O_3 of 4N purity were used. These were weighted in the corresponding nominal cationic ratios. Mixed powders were charged in a Ir crucible and molten with a 30 kW RF generator. [1 1 1] oriented yttrium−aluminum garnet single crystals were used as seeds. The pulling and rotation rates were fixed to 1 mm/h and 10 rpm, respectively.

Chemical composition was measured by inductively coupled plasma (ICP) atomic emission spectrometry with an IRIS Advantage from Nippon Jarrell-Ash Co., Ltd. X-ray diffraction data were recorded on a Rigaku 2000 diffractometer using the CuK_α line ($\lambda = 1.5418$), between $7° < 2\Theta < 140°$, a step of 0.008°, and a scan rate of 0.112°/min. The RR were performed using the program FULLPROF. A Le Bail refinement was carried out to obtain initial values for the profile parameters, using pseudo-Voigt profiles for peak shapes. The background subtraction was estimated by linear interpolation from selected refinable points. The Berar function has been used to take into account the asymmetry due to axial divergence of the diffracted beam at low angles ($2\Theta < 80°$) without any additional constraints.

Transmittance spectra were acquired with a Pekin-Elmer Lambda 90 UV/visible/NIR. Faraday rotation angles were measured with two lasers emitting at three wavelengths 532, 633, and 1064 nm. The magnetic field intensity was adjusted to ≈0.42 T.

Results and Discussion

$Tb_3Sc_2Al_3O_{12}$ Crystal. The photograph of the first crystal grown, namely, $Tb_3Sc_2Al_3O_{12}$ (TSAG), is shown in Figure 1 together with the brownish melt remaining in the Ir-crucible. The crystal is transparent with a very slight yellowish coloration and shows the typical hexagonal shape of 3-fold symmetry axis. The growing crystal separated from the melt by itself even though the growth conditions seemed to be very stable. Powder X-ray analysis of the remaining melt in the crucible indicated the coexistence of two high temperature perovskite phases, as shown in Figure 2. The peaks related to the $TbAlO_3$ phase are slightly shifted to smaller 2Θ angles, while the peaks associated to $TbScO_3$ shifted to larger angles. This is indicative of some cationic mixing in both crystallographic

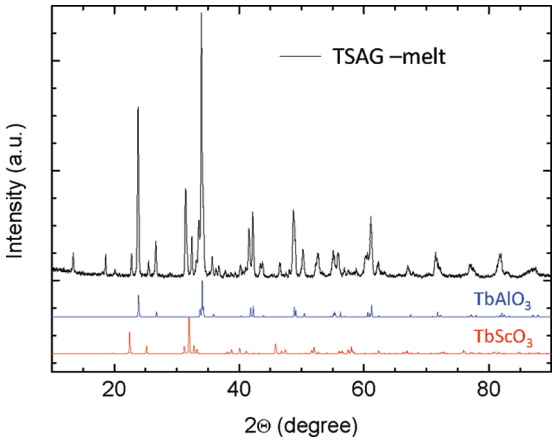

Figure 2. Powder X-ray diffraction pattern of the remaining melt from the growth of $Tb_3Sc_2Al_3O_{12}$ together with the simulated patterns for perovskites $TbAlO_3$ and $TbScO_3$.

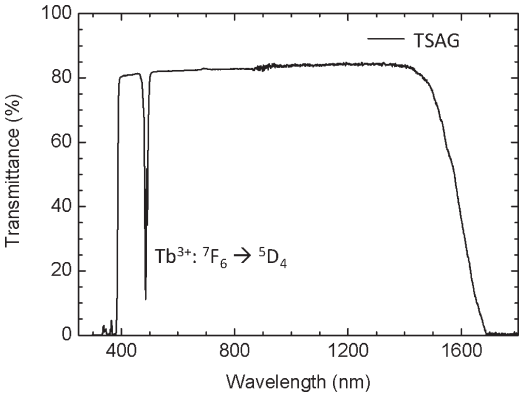

Figure 3. Transmittance spectrum of the $Tb_3Sc_2Al_3O_{12}$ crystal from Figure 1 (13 mm thick, without antireflection coating).

phases. The substitution of some Al atoms by larger Sc ones ($TbAl_{1-\delta}Sc_\delta O_3$) increases the lattice parameters and therefore decreases the reflection angles. Analogously, the substitution of Sc by the smaller Al ($TbSc_{1-\varepsilon}Al_\varepsilon O_3$) yields to larger reflection angles. The formation of these phases indicates that the melt composition has shifted from the original stoichiometric one due to the different segregation coefficients of the involved cations.

The transmittance spectrum of TSAG is given in Figure 3. It shows a high transparency from the absorption edge in the violet at 382 nm until the near IR cutoff at 1690 nm. It presents the characteristic absorption of Tb^{3+} caused by the transition $^7F_6 \rightarrow {}^5D_4$ at 486 nm. The high degree of transmittance observed in the whole visible wavelength region is quite remarkable in comparison with the transmittance of TGG, as it will be seen below in Figure 7.

The powder X-ray diffraction pattern of the TSAG crystal shown in Figure 1 is displayed in Figure 4. The RR indicates unambiguously the existence of the garnet structure with the space group $Ia\bar{3}d$. The atomic positions are summarized in Table 1. Each cation occupies the expected cationic site according to the atomic radius, that is, $\{Tb_3\}[Sc_2](Al_3)O_{12}$. Terbium, with the largest ionic radius, enters in the dodecahedral site ($Tb_8^{3+} = 104$ pm), scandium ($Sc_6^{3+} = 75$ and $Sc_8^{3+} = 87$ pm) occupies preferentially the octahedral site, and aluminum ($Al_4^{3+} = 39$ and $Al_6^{3+} = 54$ pm) localizes mainly in the smallest tetrahedral site. The RR excludes the incorporation of Sc^{3+}

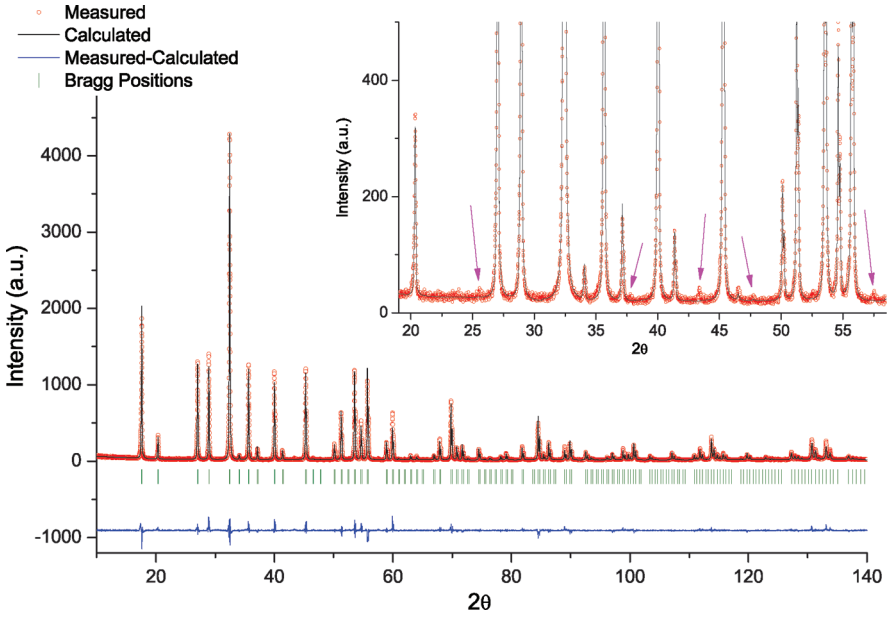

Figure 4. Rietveld refinement of the X-ray powder diffraction pattern from the $Tb_3Sc_2Al_3O_{12}$ crystal at room temperature.

Table 1. Atomic Positions According to Rietveld Refinement for the $Tb_3Sc_2Al_3O_{12}$ Crystal

atom	Wyckoff	x	y	z	B_{ISO}	occupation
Tb	24c	0.125(0)	0.0	0.25(0)	0.383(10)	0.93
Sc	16a	0.00(0)	0.0	0.00(0)	1.035(38)	0.92
Al	24d	0.375(0)	0.0	0.25(0)	0.662(48)	0.99
O	96 h	−0.03304(17)	0.04960(21)	0.15729(19)	1.496(108)	1.05

and Al^{3+} in the dodecahedral site, as well as the location of Tb^{3+} in the others, but indicates some possibility for the exchange of Sc^{3+} and Al^{3+} in their respective sites. These conclusions from our RR are in very good agreement with previous ones found in other scandium-garnets.[14] Besides the Bragg contributions of the garnet, few additional low intensive peaks were observed in the diffraction pattern (see inset in Figure 4), which could not be attributed to any of the related ternary nor binary compounds. These peaks might be caused by a marginal secondary phase, which can be related with the slight cation occupation disorder observed in the garnet structure.

The atomic distances obtained after RR indicate a regular spacing between cations and oxygen atoms: Tb−O 8 × 2.342, Sc−O 6 × 2.075, and Al−O 4 × 1.724. The effective valence of each cation (V_{Cat}) can be calculated by the bond valence (BVS) sum[15] using the equation

$$V_{Cat} = \sum_{Cat-O} V_{Cat-O} = \sum_{Cat-O} \exp\left[\frac{R_o - R_{Cat-O}}{b}\right] \quad (1)$$

where R_{Cat-O} is the cation−oxygen distance, R_o is average distance, and b is a constant equal to 0.37. The BVS calculation for the $Tb_3Sc_2Al_3O_{12}$ crystals yields the following values: V_{Tb} = 3.624, V_{Sc} = 3.254, and V_{Al} = 2.841 (see Table 4). Taking into account that the ideal valence of all three cations is 3, the estimated values by BVS indicate that Tb−O and Sc−O bonds are compressed, while on the contrary Al−O ones are stretched. This fact hints to a deficient equilibrium between the cationic sizes for the pure stoichiometric composition, which could be an important factor in determining the segregation coefficient of the cations and the previously mentioned cationic disorder between the octahedral and tetrahedral sites.

The results presented so far indicate TSAG crystals can be grown by the Cz technique, in contrast to the difficulties encountered with the primary TAG. It is seen, however, that the growth of homogeneous TSAG crystals is hindered by nonuniform segregation of the cations in the crystal. This segregation leads (a) to a limited TSAG crystal size due to the appearance of perovskites phases, and (b) to a slight gradation of material properties along the growth axis. Taking everything into account, it can be said that TSAG crystals, in spite of Cz-growth and even though they exhibit optical properties comparable to those of TAG crystals,[16] do not satisfy the requirements for a potential use in commercial FIs.

$\{Tb_3\}[Sc_{2-x}Lu_x](Al_3)O_{12}$ Crystals. In order to stabilize the growth and with it to improve the uniformity of the crystals, we aimed for the partial substitution of Sc^{3+} atoms by Lu^{3+} ones in the octahedral site. The objective of this atomic exchange would be to effectively equilibrate the descompensation of interatomic distances found by the BVS calculation (Table 4). Three $\{Tb_3\}[Sc_{2-x}Lu_x](Al_3)O_{12}$ crystals (TSLAG-1, -2, and -3)) with increasing Lu concentration ([Lu] = Lu/(Lu + Sc)) were grown by the Cz-technique under similar experimental conditions to the TSAG crystal. The photograph of the TSLAG-1 crystal is shown in Figure 5. We observed that even by the incorporation of a relatively small amount of Lu^{3+} ([Lu] = 5%) into TSAG a larger crystal could be pulled up and terminated in a regular way by a cone. In comparison with TSAG, this crystal did not show any tendency to crack and could be easily cut and processed. The thermal expansion of this crystal between room temperature and 1000 °C is shown in Figure 6. The lattice expansion is very linear over the considered temperature range, analogous to that of TSAG, with a thermal expansion coefficient of 7.92×10^{-5} K^{-1}.

All three TSLAG crystals present a slight yellowish coloration, and their transmittance spectra are shown in Figure 7

with the reference crystal for FIs TGG. For small [Lu] values, the transmittance is comparable to that of TSAG, shown in Figure 3. As the [Lu] increases, a gradual absorption increment is observed in the visible wavelength region. The most remarkable feature is the important enhancement of the transmittance in the visible region compared with the TGG crystal, which enables the use of TSLAG crystals also at wavelengths where TGG cannot be used.

The detailed analysis of the crystalline nature of TSLAG crystals by the RR indicated that all of them exhibit the same

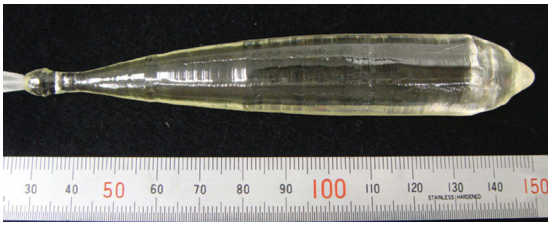

Figure 5. Photograph of the $\{Tb_3\}[Sc_{2-x}Lu_x](Al_3)O_{12}$ ($x = 0.05$) single crystal.

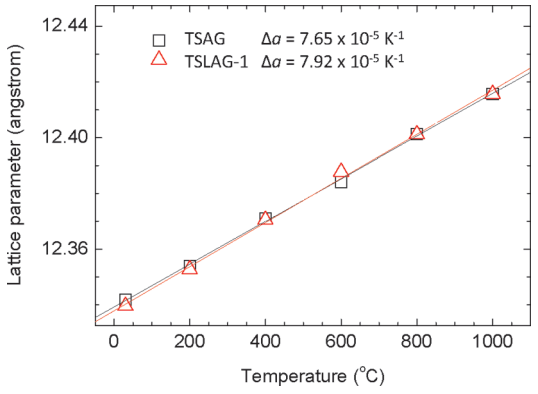

Figure 6. Lattice expansion of $Tb_3Sc_2Al_3O_{12}$ and $\{Tb_3\}[Sc_{2-x}Lu_x](Al_3)O_{12}$ ($x = 0.05$) single crystals.

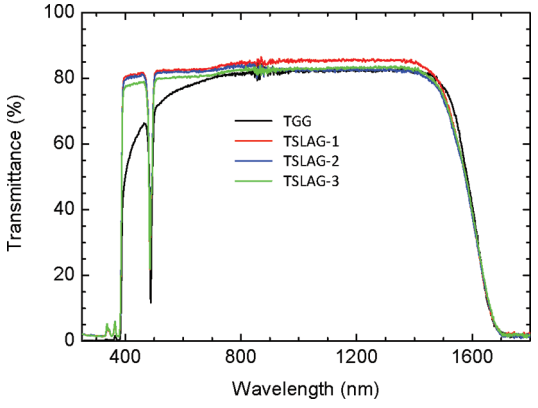

Figure 7. Transmittance spectrum of TSLAG crystals in comparison with the transmittance of TGG (12 mm thick, without antireflection coating).

garnet structure, very similar to the case of TSAG shown in Figure 4. The RR converged again to satisfying agreement factors, $R_B \approx 5-6$, $\chi^2 \approx 1.3$. The calculated lattice parameter a and the composition of TSLAG crystals are given in Table 2 together with those of the TSAG crystal. The addition of a small amount of Lu^{3+} induces an increase of the lattice parameter a as a consequence of its larger ionic radius. There is however no remarkable change in the lattice expansion coefficient up to high temperatures. The RR turned out that the contributions from Sc^{3+} and Lu^{3+} cannot be unequivocally distinguished. Both Sc^{3+} and Lu^{3+} enter primarily at the octahedral site, but as in the case of the TSAG crystal, some mixing with Al^{3+} cannot be ruled out. Further, while the concentrations of Tb^{3+} and Al^{3+} are equal and keep constant, their relative concentrations to the cations in the octahedral site (Lu + Sc) diminishes with the increase of Lu^{3+}. Three possible charge compensation mechanisms can be considered (a) the mixing of Tb^{3+} and/or Al^{3+} in the octahedral site, (b) the partial oxidation of Tb atoms to Tb^{4+}, and (c) the presence of oxygen vacancies V_O. The present results cannot elucidate the contribution of each mechanism, and further detailed characterization will be needed. The most probable is the existence of V_O together with a small concentration of Tb^{4+}, so that the actual formulation of the TSLAG compounds should be more accurately expressed as $\{Tb_3\}[Sc_{2-x-y}Lu_xAl_y](Al_{3-p-r}Sc_pLu_r)O_{12-s}V_{Os}$. In order to elucidate more accurately the distribution and disordering of Sc^{3+} and Lu^{3+} ions among cationic sites in the mixed TSLAG crystals, local-structure sensitive measurements should be carried out, for example nuclear magnetic resonance with the isotopes ^{27}Al and ^{45}Sc.[14]

The results of the ICP chemical composition analysis given in Table 3 for the TSLAG crystals indicate that Sc^{3+} and Lu^{3+} are present in the crystal in the corresponding stoichiometric composition. A comparison with the RR in Table 2 show that (a) TSAG has a small Al excess or Tb deficiency, (b) the segregation coefficient of Lu is larger than that of Sc, and (c) above a certain [Lu] (< 5%) small amounts of Sc and Lu are incorporated in the crystal as a residual byproduct apart from the garnet phase. These byproducts could not be formally identified by X-ray analysis, except for one sample with apparently slight traces of $TbAlO_3$. The increment of such traces with the increase of [Lu] could be the origin for the increasing transmittance losses in the visible wavelength region (Figure 7).

BVS calculations for the TSLAG crystals are summarized in Table 4 together with the one for TSAG. It is seen that by the incorporation of a small amount of Lu^{3+} (TSLAG-1) the Tb−O, Sc−O, and Al−O bonds are stretched in comparison

Table 3. ICP Analysis of $\{Tb_3\}[Sc_{2-x}Lu_x](Al_3)O_{12}$ Crystals

crystal	composition	(Lu + Sc)	[Lu] (%)	$[Lu]_{nominal}$ (%)
TSAG	$Tb_{2.99}Sc_{1.93}Al_{3.16}O_{12}$	1.93		
TSLAG-1	$Tb_{2.96}Sc_{1.95}Lu_{0.09}Al_{2.97}O_{12}$	2.04	4.56	2.5
TSLAG-2	$Tb_{2.96}Sc_{1.97}Lu_{0.13}Al_{2.95}O_{12}$	2.10	6.08	5
TSLAG-3	$Tb_{2.95}Sc_{1.96}Lu_{0.21}Al_{2.98}O_{12}$	2.16	9.56	10

Table 2. Rietveld Refinement of $\{Tb_3\}[Sc_{2-x}Lu_x](Al_3)O_{12}$ Crystals

crystal	a (Å)	Δa ($\times 10^{-5}$ K^{-1})	composition	(Lu + Sc)	[Lu] (%)	$[Lu]_{nominal}$ (%)
TSAG	12.339	7.65	$Tb_{3.00}Sc_{1.96}Al_{3.13}O_{12.1}$	1.96		
TSLAG-1	12.340	7.92	$Tb_{3.00}Sc_{1.87}Lu_{0.10}Al_{2.96}O_{11.9}$	1.97	5.08	2.5
TSLAG-2	12.355	7.68	$Tb_{3.00}Sc_{1.63}Lu_{0.10}Al_{2.96}O_{11.5}$	1.72	5.58	5
TSLAG-3	12.351	7.61	$Tb_{3.00}Sc_{1.28}Lu_{0.20}Al_{3.00}O_{11.2}$	1.49	13.68	10

Table 4. Bond Valence Sum of Cations in $\{Tb_3\}[Sc_{2-x}Lu_x](Al_3)O_{12}$ Crystals

crystal	Tb−O	V_{Tb}[a]	Sc−O	V_{Sc}[a]	Al−O (%)	V_{Al}[a]
TSAG	8 × 2.342	3.624	6 × 2.075(3)	3.257	4 × 1.724(3)	2.841
TSLAG-1	4 × 2.357(3), 4 × 2.464(3)	3.043	6 × 2.080(4)	3.214	4 × 1.774(3)	2.638
TSLAG-2	4 × 2.332(2), 4 × 2.548(2)	2.900	6 × 2.088(2)	3.145	4 × 1.719(2)	3.061
TSLAG-3	4 × 2.365(2), 4 × 2.500(2)	2.885	6 × 2.078(2)	3.231	4 × 1.745(2)	2.853

[a] According to eq 1, and the values $R_{o_{Tb}} = 2.049$, $R_{o_{Sc}} = 1.849$, and $R_{o_{Al}} = 1.620$.

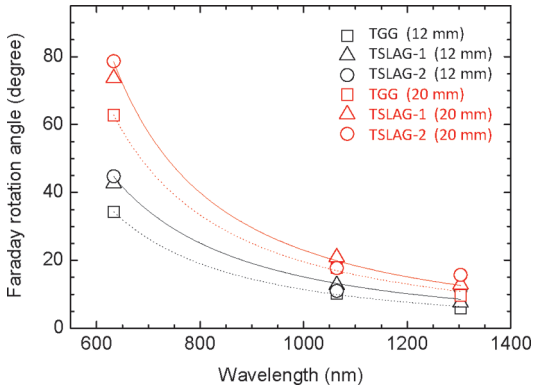

Figure 8. Faraday rotation angles of TSLAG crystals as a function of the wavelength λ and the sample length (12 and 20 mm). A TGG crystal was measured as reference, and the measured data were fitted by a equation in the form $A/(\lambda^2 - \lambda_o^2)$, with A and λ_o constants.

with TSAG. In contrast, TSLAG-2 presents shorter cationic bonds than TSLAG-1. Taking everything into account, a minimum deviation from the ideal cationic valence 3 could be somewhere between 2 and 5% [Lu]. This estimation is in good agreement with the previous discussion, where the appropiate [Lu] to obtain a stoichiometric composition of the garnet phase is envisaged in the same concentration range. Consequently, present results suggest that by the partial substitution of Sc^{3+} by Lu^{3+}, it is possible to congruently grow TSLAG crystals with uniform properties.

The magneto-optical response of TSLAG crystals is shown in Figure 8 as a function of the wavelength and light path, and in comparison with the reference material TGG. The Faraday rotation angles of TSLAG crystals are between 25 and 35% larger than those of TGG samples. These results are very similar to those reported for TAG crystals and $Tb_3Ga_{5-x}Al_xO_{12}$ mixed crystals.[9,16] A theoretical interpretation of the increase in Faraday rotation will require further experiments concerning detailed crystal field analysis and quantum based superexchange interaction, so that the Tb^{3+} electric dipole transitions in this host can be estimated.

Conclusion

Summarizing, large $Tb_3Sc_2Al_3O_{12}$ and $\{Tb_3\}[Sc_{2-x}Lu_x](Al_3)O_{12}$ single crystals could be grown by the Cz technique. By RR, it is demonstrated that these crystals crystallize in the garnet structure with space group $Ia\bar{3}d$. As expected, isovalent substitution of Sc^{3+} by Lu^{3+} is achieved at the octahedral site, although a slight mixing among the cationic sites cannot be ruled out, as in the case of pure TSAG crystals. The substitution Lu_{Sc} improves the total balance of cationic sizes, favoring the homogeneity and stability of the grown crystals. TSLAG crystals yield a Faraday rotation comparable to that of TAG crystal, while at the same time show an improved transparency in the visible wavelength region. Presented results indicate therefore that TSLAG crystals exhibit better properties than commercial TGG crystals. In conclusion, TSLAG crystals are promising candidates for FI applications in the visible-near IR wavelength region.

Acknowledgment. The authors would like to express their sincere thanks to Mr. S. Ichikawa from Fujikura Co., Ltd. for the ICP analysis and to Kogakugiken Co., Ltd. for the Faraday rotation measurements. This research was partially supported by the Ministry of Education, Science, Sports and Culture, Grant-in-Aid for Scientific Research (C), 22560316, 2010.

References

(1) Mukimov, K. M.; Sokolov, B. Y.; Valiev, U. V. *Phys. Stat. Sol. (a)* **1990**, *119*, 307.
(2) Crossley, W. A.; Cooper, R. W.; Page, J. L. *Phys. Rev.* **1969**, *181*, 896.
(3) Yang, J. H.; Xu, Y.; Zhang, G. Y. *J. Phys. Phys.* **1994**, *75*, 6798.
(4) Geho, M.; Sekijima, T.; Fujii, T. *J. Cryst. Growth* **2005**, *275*, e663.
(5) Rubinstein, C. B.; Uitert, L. G. V.; Grodkiewicz, W. H. *J. Appl. Phys.* **1964**, *35*, 3069.
(6) Ganschow, S.; Klimm, D.; Reiche, P.; Uecker, R. *Cryst. Res. Technol.* **1999**, *34*, 615.
(7) Khazanov, E. A.; Mukhin, I. B.; Palashov, O. V.; Voytovich, A. V.; Zheleznov, D. S. Proceedings of the Lasers and Electro-Optics, 2008 and 2008 Conference on Quantum Electronics and LaserScience CLEO/QELS, San Jose, CA, May 4−9, **2008**; IEEE: New York, **2008**.
(8) Linares, R. *Solid State Commun.* **1964**, *2*, 229.
(9) Zhang, W.; Guo, F.; Chen, J. *J. Cryst. Growth* **2007**, *306*, 195.
(10) Kokta, M. *J. Solid State Chem.* **1973**, *8*, 39.
(11) Allik, T. H.; Morrison, C. A.; Gruber, J. G.; Kokta, M. R. *Phys. Rev. B* **1990**, *41*, 21.
(12) Suchow, L.; Kokta, M.; Flynn, V. *J. Solid State Chem.* **1970**, *2*, 137.
(13) Suchow, L.; Kokta, M. *J. Solid State Chem.* **1972**, *5*, 85.
(14) Tien, C.; Charnaya, E. V.; Sun, S. Y.; Wu, R. R.; Ivanov, S. N.; Khazanov, E. N. *Phys. Status Solidi B* **2002**, *233*, 222.
(15) Brown, I. D. *Chem. Rev.* **2009**, *109*, 6858.
(16) Geho, M.; Sekijima, T.; Fujii, T. *J. Cryst. Growth* **2004**, *267*, 188.